

## **3D Modeling of of Distribution Andesite and Breccia Rocks Using Geoelectric Resistivity in Potential Areas of Minerals in Madiun Regency, Indonesia**

**Rizqi Prastowo\***Department of Mining Engineering,  
Institut Teknologi Nasional Yogyakarta  
INDONESIA**Setyo Pambudi**Department of Geology Engineering,  
Institut Teknologi Nasional Yogyakarta  
INDONESIA**Al Hussein Flowers Rizqi**Department of Geology Engineering, Institut  
Teknologi Nasional Yogyakarta  
INDONESIA**Vico Luthfi Ipmawan**Department of Physics,  
Institut Teknologi Sumatera,  
INDONESIA**Dyah Arum Arimurti**Department of Physics Education,  
Jember University  
INDONESIA**Berwyn Dzaky Radhitya**Department of Geosciences,  
University of Tsukuba,  
JAPAN**\*Correspondence: E-mail:** [rizqi@itny.ac.id](mailto:rizqi@itny.ac.id)

---

**Article Info****Article history:**

Received: February 10, 2024

Revised: May 15, 2024

Accepted: June 28, 2024



**Copyright :** © 2024 Foundae (Foundation of Advanced Education). Submitted for possible open access publication under the terms and conditions of the Creative Commons Attribution - ShareAlike 4.0 International License (CC BY SA) license (<https://creativecommons.org/licenses/by-sa/4.0/>).

---

**Abstract**

This research focuses on the distribution of andesite and breccia rocks in East Java, Indonesia, specifically in Morang Village, Madiun Regency, through geoelectric resistivity measurements. This study aims to enhance geoelectric interpretation from 2D to 3D, providing high accuracy in target positioning for potential building material resources. By employing a dipole-dipole configuration with electrode spacing, the resistivity values of subsurface rocks were analyzed to classify the types and distributions of building materials, such as andesite and breccia. Data was collected through field measurements and geological surveys, followed by inverse modeling using the least squares method. The results reveal that andesite, with resistivity values above 1000  $\Omega$ m, is distributed predominantly in the southeast-northwest trend at a depth of 10–15 meters, while breccia, with resistivity values between 600–900  $\Omega$ m, is found at various depths closer to the surface. The geological interpretation suggests that the southeast-northwest orientation may correlate with an ancient basin structure, which directed lava flow during past volcanic activities, forming these rock layers. This study contributes valuable information for local infrastructure planning by providing data on accessible rock resources essential for construction. The application of the 3D geoelectric model offers an effective tool for environmental assessment and mineral exploration, promoting sustainable resource management.

**Keywords:** 3D modeling; geoelectric resistivity; andesite distribution; breccia formation; exploration

---

**To cite this article:** Prastowo, R., Pambudi, S., Rizqi, A, H, F., Ipmawan, V, L. Arimurti, D, A. and Radhitya, B, D. (2024). 3D Modeling of of Distribution Andesite and Breccia Rocks Using Geoelectric Resistivity in Potential Areas of Minerals in Madiun Regency, Indonesia. *International Journal of Hydrological and Environmental for Sustainability*, 3(2), 89-101. <https://doi.org/10.58524/ijhes.v3i2.474>

---

## **INTRODUCTION**

The era of globalization especially the Industrial Revolution 4.0 has demanded various countries to continue to develop the potential of natural resources (Mibei, 2014; Watlet et al., 2020). Indonesia is one of the developing countries in the world that has abundant natural resources. But the natural wealth cannot be explored properly and maximally. Various problems arise, due to exploration that

are not balanced with rehabilitation. The impact of this exploration is very much felt by Indonesia, even the world. One of the most important things in exploration is science in the field of geosciences (Bronto et al., 2012; Khalil & Santos, 2011; Oskooi & Abedi, 2015).

The importance of the science of geoscience for developing countries is to be able to help provide information about which areas have the potential manifestation of materials or building materials (Thoreau & Prayer, 2000). As we know, various developing countries continue to increase infrastructure development such as office buildings, roads, transportation, and so on. However, the development project can run slowly, if not the availability of building materials, especially in Indonesia (Saparun et al., 2022; Schuessler et al., 2016).

One of the inhibiting factors of the Dinas Pekerjaan Umum (DPU) or Public Works Agency and Tata Ruang Kota (TRK) or City Spatial Planning in Indonesia, especially in the city of Madiun, is that the bridge infrastructure that connects the city of Madiun with the surrounding area has not been integrated. This must be realized to fulfill Madiun's DPU and TRK vision, namely "Realizing the Quality of Infrastructure Networks that Are Strong for Supporting the City of Madiun that is More Advanced and Prosperous".

Based on the vision of the Office of Public Works and Spatial Planning of the City of Madiun, the realization of this problem is balanced with the availability of development materials to support the implementation of the development. One important material is mountain rock (Muthamilselvan et al., 2019). Examples of mountain rocks are andesite, breccia, agglomerates, etc (Chen et al., 2020). Stone mountain is one type of volcanic igneous rock that is widely used in the field of construction such as building foundation raw materials, paving roads and making bridges (Tang et al., 2021). Economic assessment of mountain rock is also viewed from its reserve resources, so an exploration method is needed that is able to reveal the presence of below-ground andesite rocks and their dispersal patterns (Hartmann et al., 2024).

Exploration of natural resources that are not supported by good science, can damage the ecosystem that is located in mining locations. The importance of initial observation without damaging the surface of the mining area is very necessary to be studied. In the era of industrial revolution 4.0, the development of science in the field of geosciences continued to be developed to assist in mapping the mining area (Nugraha et al., 2019). Not only that, the interpretation process is very important to describe how rock formations in a region. This interpretation can be made in 2-dimensional (2D) or 3-dimensional (3D) forms (Trian et al., 2021).

Geophysical exploration is one of the sciences in the field of geosciences. Geophysical exploration can assist in the process of geological mapping, potential mining areas, knowing disaster-prone areas, and so on (Czinder & Török, 2021). One of the geophysical methods that can be used to determine the potential area of a building material or material is the Geoelectric method (Gan et al., 2017; Nurwidianto & Yuliyanto, 2022; Saparun et al., 2022).

Geoelectric method is one of the geophysical methods that utilizes the electrical properties of rocks, namely rock resistivity. Basically rocks are bad / resistive conductors of electricity, but rocks have different properties and compositions which result in variations in resistivity values (Anthony, 2017; Muthamilselvan et al., 2019; Taira, 2001). Resistivity value is used to distinguish between one type of rock and another. 3D Dimension (3D) modeling of rock resistivity using the Geoelectric Method is expected to provide an overview of the pattern of mountain rock distribution (Chambers et al., 2022).

Rock resistivity is the value of the electrical inhibition of a rock. The greater the resistivity value of the rock, the smaller the current value that can flow in a conductor, and vice versa (Adejumo et al., 2018; Alonso-Pandavanes et al., 2023; Listyani et al., 2023; Sujitapan et al., 2024; Xu & Wang, 2021). The resistivity values of rocks vary, the formulates resistivity in **Table 1** as follows:

**Table 1.** Material variations of the earth (rocks) (Nugraha et al., 2019)

| No | Name of rock              | Resistivity ( $\Omega\text{m}$ ) |
|----|---------------------------|----------------------------------|
| 1  | Air                       | 0                                |
| 2  | Clay                      | 1 – 100                          |
| 3  | Ground Water              | 0.5 – 300                        |
| 4  | Old Breccia / Gravel      | 100 – 600                        |
| 5  | Old Andesite / Dry Gravel | 600 – 10.000                     |

Geoelectric is a method in geophysics that studies the nature of electricity in the earth and how to detect it on the surface of the earth. This detection includes the measurement of potential differences, currents, and electromagnetics that occur naturally or due to the injection of currents into the earth (Muthamilselvan et al., 2019; Saparun et al., 2022). The geoelectric method can be used properly if there is contrast resistivity between mediums. Contrast can be a relatively conductive medium to a non-conductive medium, or there are differences in lithology (Muthamilselvan et al., 2019).

The simple approach to obtaining type resistance for every rock beneath the earth's surface is to assume that the earth is a isotropic homogeneous medium. If an electric current with a  $J$  current is flowed into the earth, then the current will spread in all directions with equal magnitude (Meju & Le, 2002). The current flow through an element of area  $A$  is written as:

$$I = J \cdot A \quad (5)$$

The relationship between current density and electric field  $E$  is expressed in Ohm's law:

$$J = \frac{1}{\rho} E \quad (6)$$

where,  $E$  = electric field (volt/meter)  $\rho$  = resistivity of medium ( $\Omega \text{m}$ ).

In isotropic homogeneous conditions, the potential at a point caused by the current flow is only determined by distance  $r$  from the current source to the measurement point (Playà et al., 2010). In this system the potential decreases throughout  $r$ , hence the magnitude of the electric field is written as,

$$E = -\nabla V = -\frac{dV}{dr} \quad (7)$$

because  $A$  is the area of half the ball written as,

$$A = 2\pi r^2 \quad (8)$$

so,

$$J = \frac{I}{2\pi r^2} \quad (9)$$

then, based on equations (6), (7) and (9), their potential can be integrated as,

$$\Delta V = \int dV = -\frac{\rho I}{2\pi} \int \frac{1}{r^2} dr = \frac{\rho I}{2\pi r} \quad (10)$$

The use of spherical area in this calculation is because for a homogeneous isotropic earth it means that there is no other layer other than the boundary plane between soil and air (Muthamilselvan et al., 2019; Nugraha et al., 2019). Air has zero type of delivery or infinite jemis resistance, so the current will only flow into the earth (Ibrahim et al., 2019; Playà et al., 2010). Based on equation (8), it appears that the surface of the equipment is in the form of a half-ball surface, while the current flow line and electric field are radially directed (Figure 1).

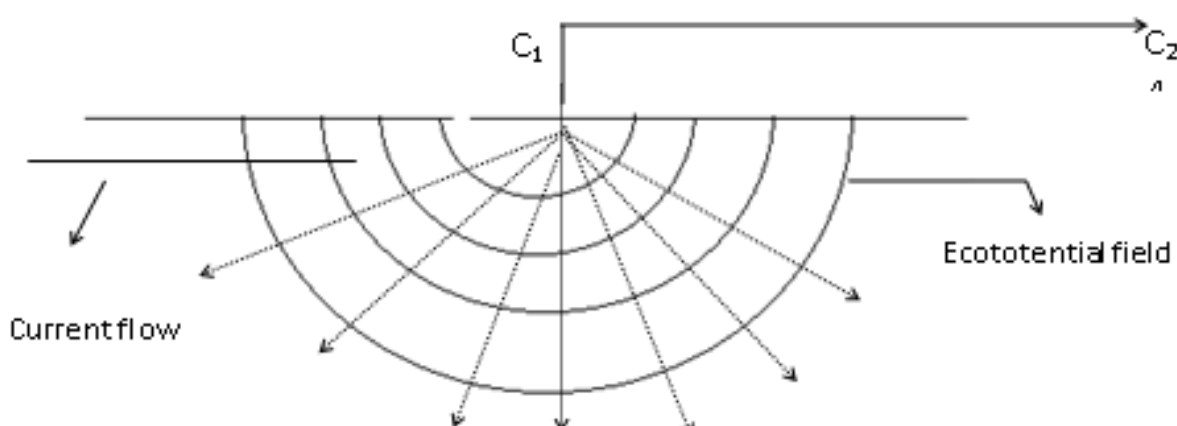


**Figure 1.** Current flow originating from a homogeneous isotropic source in the earth

## METHOD

This study aims to: 1. Develop geoelectric interpretation from 2D to 3D, with a very good level of target positioning accuracy. 3D interpretation of resistivity of building materials in the area of Morang Village, Kec. Kare, Kab. Madiun, East Java, Indonesia. 2. Provide information to the DPU, TRK, and the government regarding the location of the area that has building materials as a form of support for the development of the country's infrastructure.

This research method includes quantitative research, where the data used is measurement data in the form of physical quantities, namely resistivity, electrical voltage, and electric current. Data in the form of numbers are processed based on theory. The retrieval of this data from the literature study in the form of geological information in the study area, and direct measurements in the field. The measurement results in the form of resistivity data are then inverted by the inversion least square method which then gets a cross section model, through this cross-sectional model then in quantitative interpretation.

The location of this research is the area of Morang Village, Kec. Kare, Kab. Madiun, Indonesia. In this study the configuration of the geoelectric method used is a dipole-dipole with both electrode spaces as large, but the space between the current electrode and the potential electrode is made larger and measured repeatedly. The stages of taking measurement data in the field are as follows **Figure 2**. Plug the electrode on the ground surface with a spacing of 20 m, and operate a 380 m cable, with the number n which is 10.

- The cable is spread out as a current and potential that connects the electrode with a resistivity meter.
- After the four electrodes are connected with resistivity meter, the measurement is ready
- Record electric current and voltage arising after the current is injected into the ground.

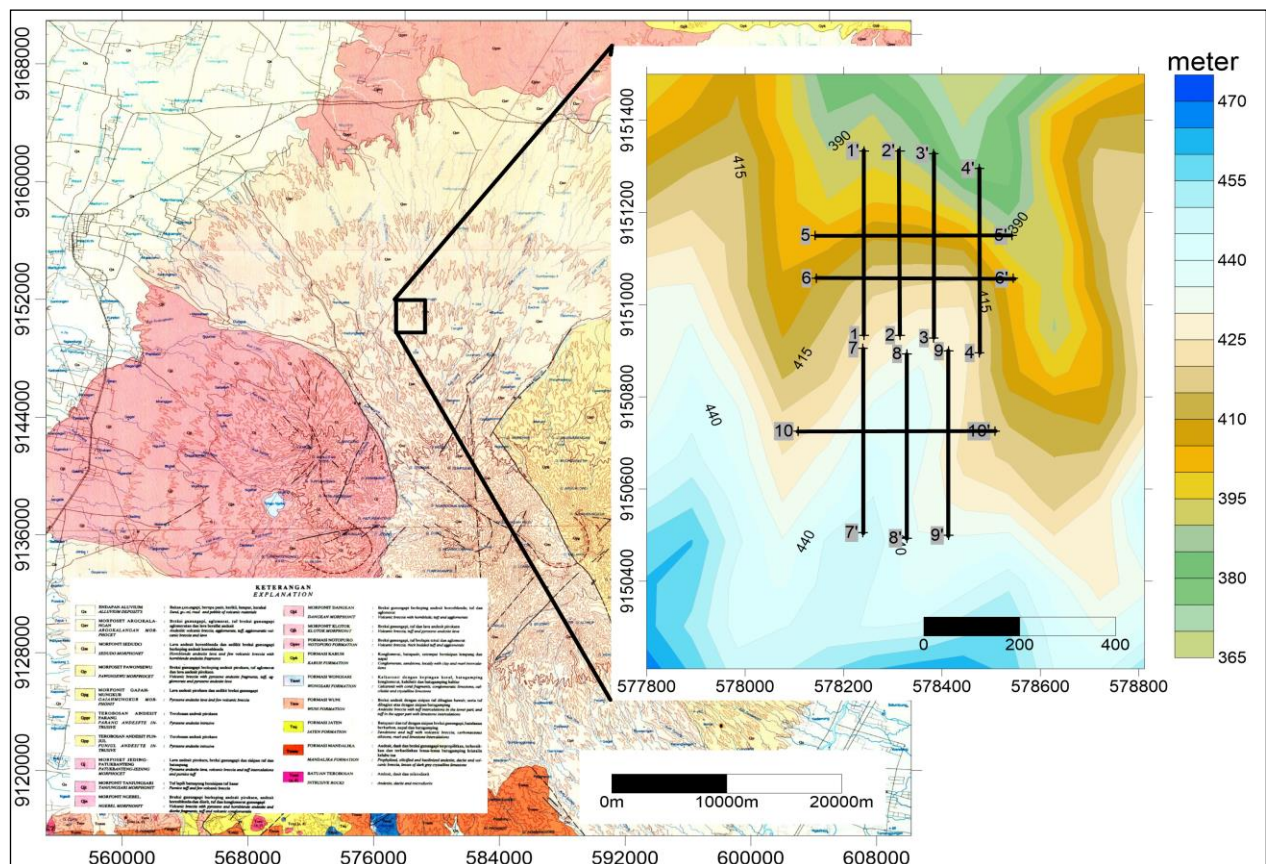


**Figure 2.** Geoelectric Research Survey Design Map

## RESULTS AND DISCUSSION

Based on the results of the final mapping analysis (Dipole-dipole Configuration) conducted with computer programs, and also with curve matching and supported by regional geological data from the study area, the final depth results are correlated with the actual type of resistivity ("True resistivity"). Based on the correlation between the data measured by resistivity and Table 1, the rocks are divided into 2 types which have quite high resistivity as follows:

1. Andesite: The resistivity value is above 1300  $\Omega\text{m}$ , consisting of quartz minerals which have a high resistivity value than other lithologies around it.
2. Breccia: The resistivity value is 600-900  $\Omega\text{m}$ , breccia rock with igneous fragments and dominant sandstone matrix.

Based on the interpretation of the inverse results shown in **Figure 3**, the response obtained resistivity value (electrical inhibitory) with a value of more than 1200  $\Omega\text{m}$  which is shown in purple in 2D display which is Andesite rock based on Table 1, resistivity value (electrical resistance) with the value of 600-900  $\Omega\text{m}$  which is shown in orange to yellow in the cross section is Breccia lithology, and the resistivity value below 500  $\Omega\text{m}$  with green to blue is the distribution of the matrix that binds between fragments is sedimentary rock (Biswas, 2018). On line 1, the breccia rock is quite large and its presence is close to the surface. Whereas Andesite rocks are close enough from the surface that is at  $\pm 20$  meters depth. The area of Andesite rocks is quite large, starting from the point 200 meters to 280 meters from the starting point of the line.

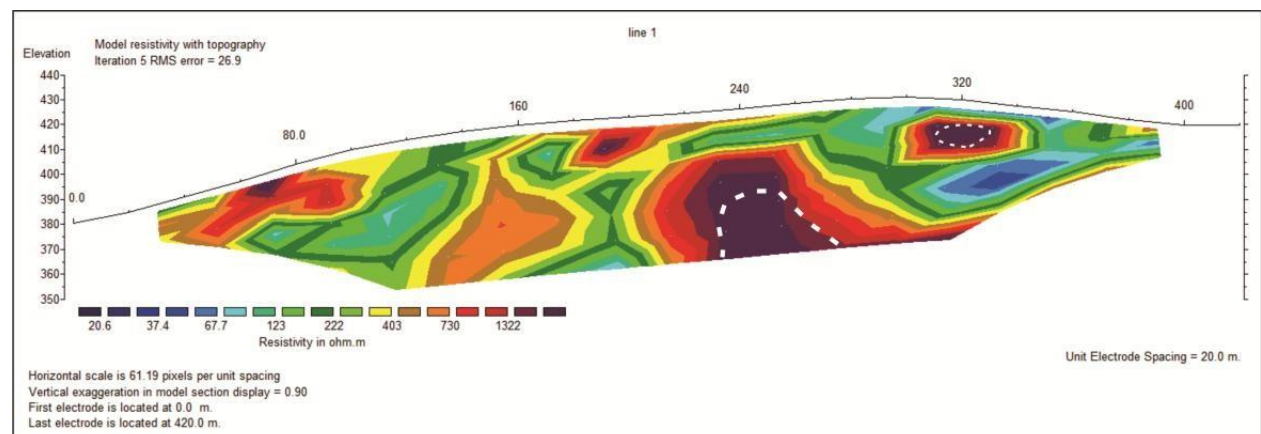


**Figure 3.** Resistivity model on line 1

In addition, the results of inversion shown in **Figure 4**, the response obtained resistivity value (electrical inhibitory) with a value above 1000  $\Omega\text{m}$  which is shown in purple in the cross section where it is Andesite, resistivity value (electrical resistance) with a value of 600-800 800m shown in orange to yellow in the cross section is Breccia. On line 2, Breccia rocks are located almost along the measurement path, but their presence is far from the ground surface with an average depth of  $\pm 20$ -50 meters. Whereas only a small amount of Andesite rocks can be seen in the results of interpretation of line 2. It is suspected that Andesite rocks have a considerable depth on line 2 which is less than  $\geq 50$  meters.

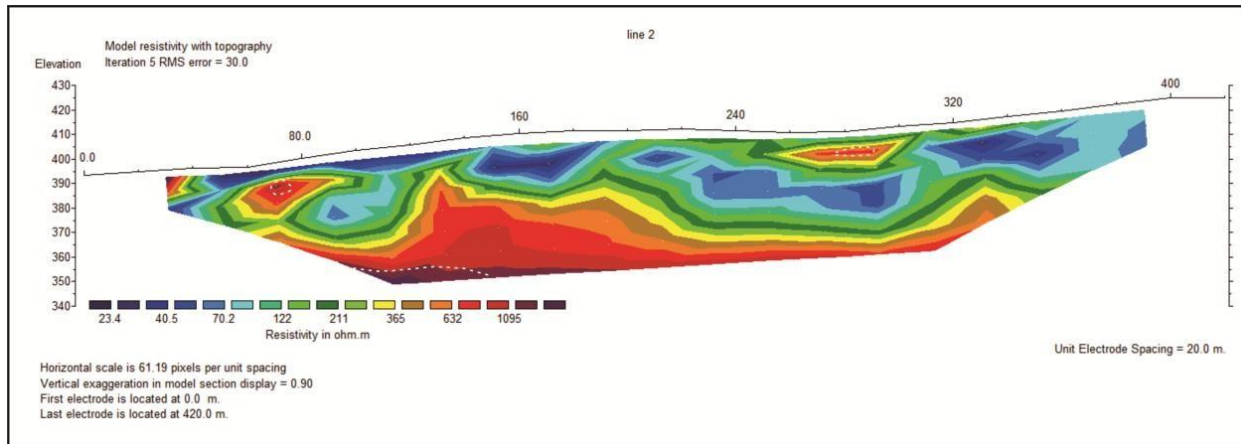


**Figure 4.** Resistivity model on line 2

In **Figure 5**, resistivity values (electrical inhibitory) 40 - 607  $\Omega$ m which are shown in blue to purple are sedimentary or soil rocks. While Breccia is seen at resistivity  $\geq 600 \mu\text{m}$ . Breccia rock on line 3, is in a deep position which is  $\pm 40$  m from the surface. The depth of the Breksi rocks is thought to be due to the geological conditions that have weathered rocks a lot, and also the presence of trees so that sedimentation in the form of soil on Breccia rocks is quite thick. The high rainfall and the intensity of the sun in Indonesia is one of the frequency factors of weathering that often occurs.

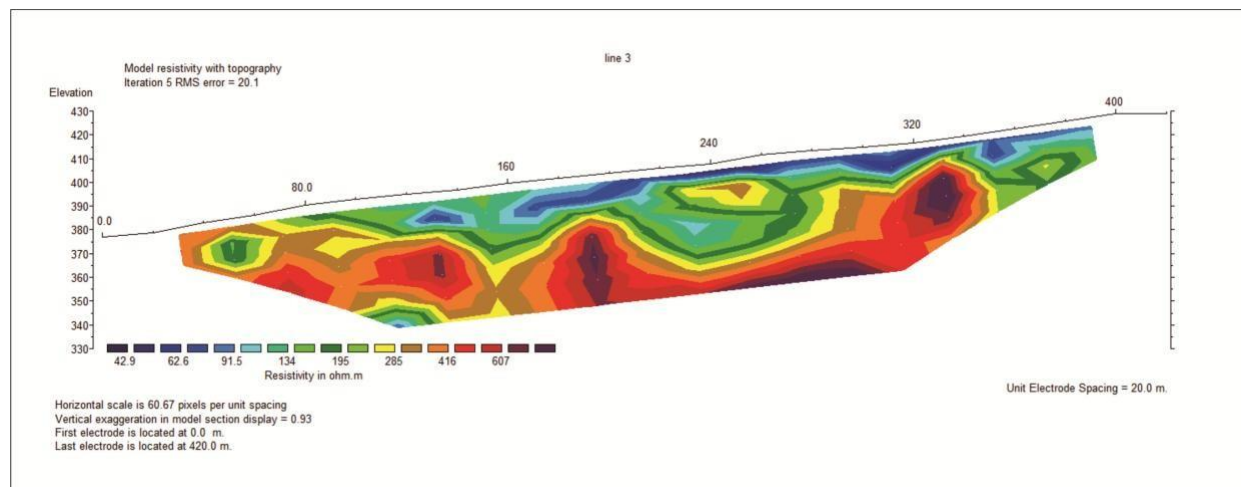


**Figure 5.** Resistivity model on line 3

For line 4, which is shown in **Figure 6**, shows a considerable amount of breccia but has a relative presence within  $\pm 30$  m. Resistivity value (electrical inhibition) with a value of more than 600  $\Omega$ m indicated by orange to purple is the lithology of Breccia. Andesite rocks on line 4 are likely to be far from the surface, so they are not seen in the results of the interpretation.

Based on the results of the inversion shown in **Figure 7**, the overall response obtained is Breccia where the resistivity value (electrical inhibitory) with a value of more than 600  $\Omega$ m is shown in blue to purple. This breccia can be seen starting at a depth of about 20-80 m. The appearance of this breccia is shown in red to purple and is at a distance of 240-320 m from the starting point of line 5. Whereas the red to bronze color which is separated from Breccia rocks is bolder from volcanic results.

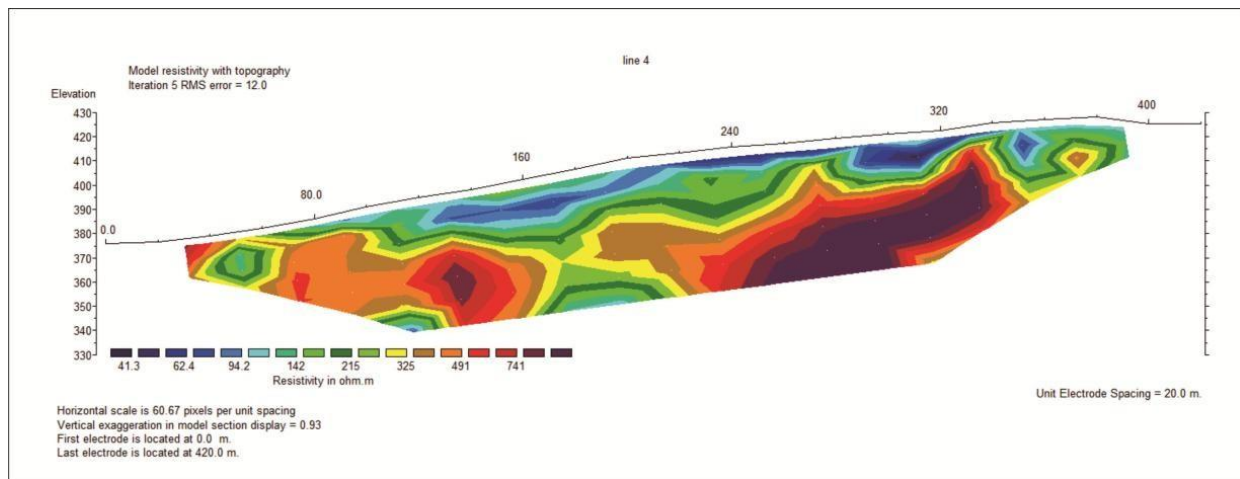


**Figure 6.** Resistivity model on line 4

Based on the results of the inversion shown in **Figure 7**, the overall response obtained is Breccia where the resistivity value (electrical inhibitory) with a value of more than 600  $\Omega\text{m}$  is shown in blue to purple. This breccia can be seen starting at a depth of about 20-80 m. The appearance of this breccia is shown in red to purple and is at a distance of 240-320 m from the starting point of line 5. Whereas the red to bronze color which is separated from Breccia rocks is bolder from volcanic results.

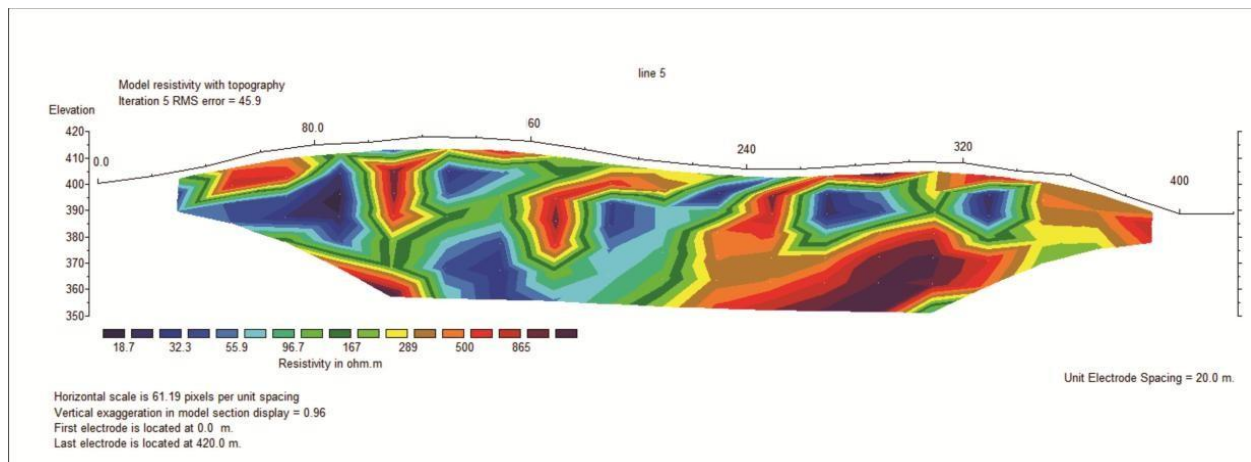


**Figure 7.** Resistivity model on line 5

Based on line 6 shown in **Figure 8** is slightly different from the previous line, the overall response obtained is the Agglomerate Unit or sedimentary rock where the resistivity value is 41-450  $\Omega\text{m}$  indicated by green to blue. While the resistivity value of more than 600  $\Omega\text{m}$  is Breccia, but the appearance of the Breccia on this 6th path is relatively small, at a depth of about  $\pm 60\text{m}$ , it is suspected that the presence of Breccia rocks leads to a deeper point.

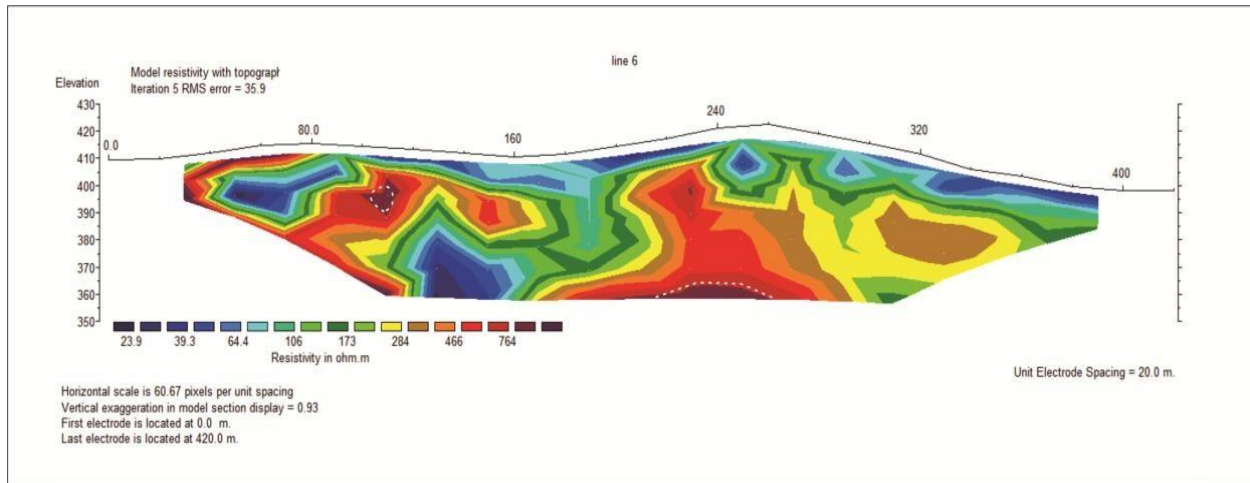


**Figure 8.** Resistivity model on line 6

Based on the results of inversion shown on Line 7 (Figure 9), the resistivity value (electrical inhibitory) with a value above 1000 showed which is shown in purple in the cross section where is an Andesite in the form of boulders, and there is no resistivity value 500-800  $\Omega\text{m}$  which is shown in orange to yellow is breccia, and the resistivity value below 300  $\Omega\text{m}$  is the distribution of the matrix that binds between fragments namely sediment or soil. On this line 7, it is seen that there are very few Andesite rocks or Breccia.

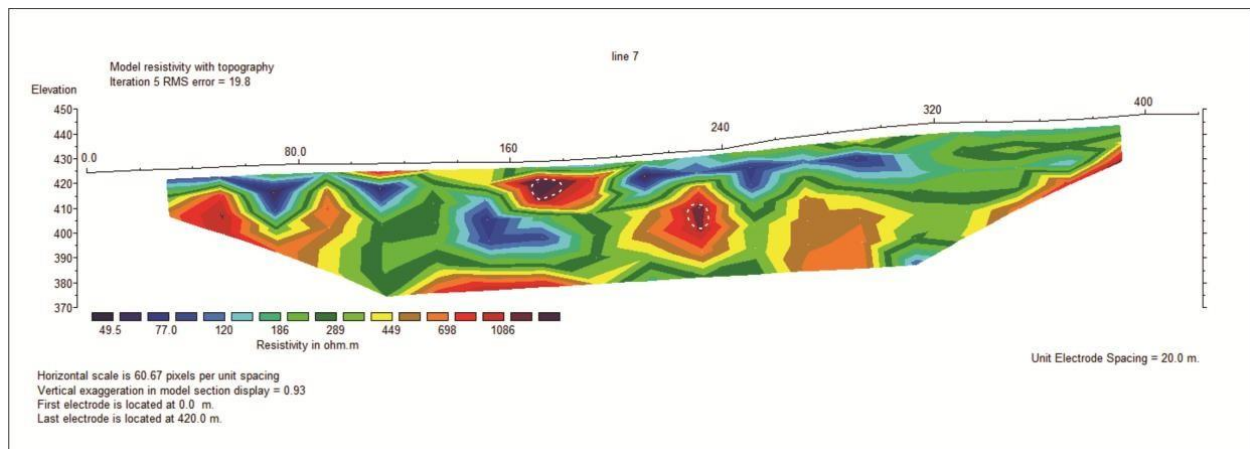


**Figure 9.** Resistivity model on line 7

Based on the results of inversion shown in Figure 10, the resistivity value (electrical inhibitory) with a value of more than 1000  $\Omega\text{m}$  indicated in purple is an Andesite rock. Andesite rocks on line 8, have a fairly shallow presence which is around  $\pm 10$  m. While the resistivity value (electrical inhibitory) with a value of 600-900  $\Omega\text{m}$  which is indicated by the young to old orange in the cross section is Breccia lithology. In the 8-section andesite trajectory tends not to show continuity to a deeper existence but only the spots, or it can be possible in the form of boulder volcanic results. While the resistivity value below 300  $\Omega\text{m}$  is the distribution of the matrix that binds between fragments in the form of soil or the results of weathering of rocks.

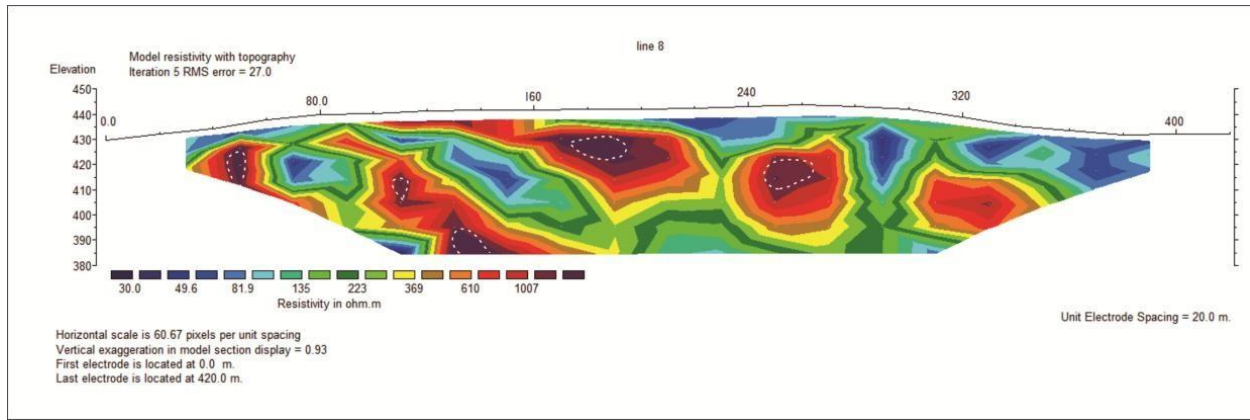


**Figure 10.** Resistivity model on line 8

Based on the results of the inversion shown in **Figure 11**, the response obtained by the resistivity value (electrical inhibitory) with a value of more than 1000  $\Omega\text{m}$  which is shown in purple in the cross section where is an Andesite. Andesite rock on Line 9, has a very shallow existence with a large enough area. While the resistivity value (electrical inhibitory) with a value of 600-900  $\Omega\text{m}$  which is indicated by the young to old orange in the cross section is Breccia lithology. Thus andesite is in the breccia fragment at a depth of about 10m and there are 3 blocks. There is 1 block that shows the continuity of Andesite resources, which are shown at a depth of about 30m.

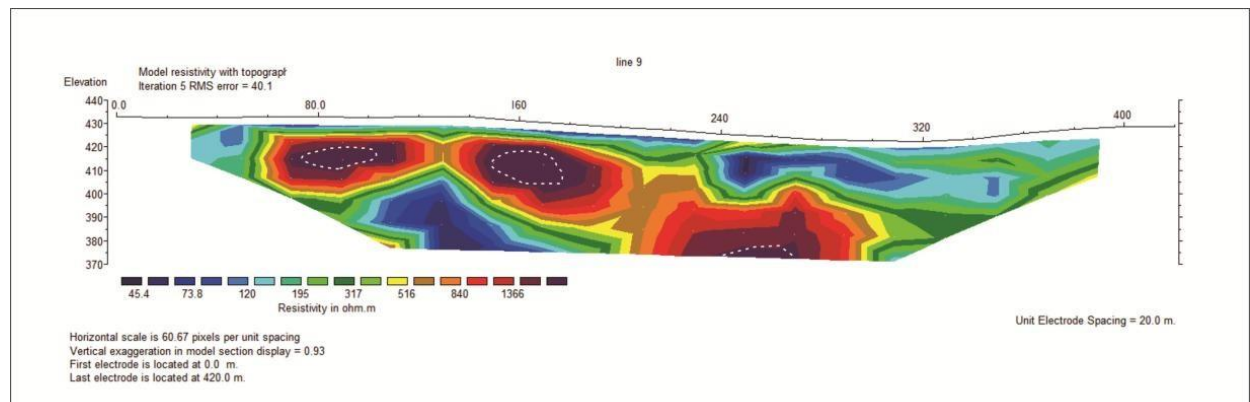


**Figure 11.** Resistivity model on line 9

Line 10 is the last trajectory in the study shown in **Figure 12**, the response obtained has a resistivity value (electrical inhibitory) with a value above 1000  $\Omega\text{m}$  indicated in purple on the cross section where it is Andesite and shows a tendency towards continuity to a deeper depth, value resistivity (electrical resistance) with a value of 600-900  $\Omega\text{m}$  which is indicated by orange to yellow in cross section is a Breccia in the form of a bloder bloder from volcanic results, and a resistivity value below 350  $\Omega\text{m}$  is the distribution of matrices that bind between fragments or soil of clay.

Based on the results of the interpretation of 10 geoelectric data in **Figure 5-14**. These results are then correlated to get 3D results. These results are then made in the form of mapping maps. The results of the dipole-dipole configuration geoelectric measurements, andesite 3D models shown in Figure 13. Based on andesite 3D models tend to widen to the southeast - northwest and spots. In the area of andesite spot, there tends to be 4 spots, namely at coordinates (578234.34, 9151220.80), (578439.97, 9150808.27), (578351.79, 9150730.73), (578454.72, 9150652.18).

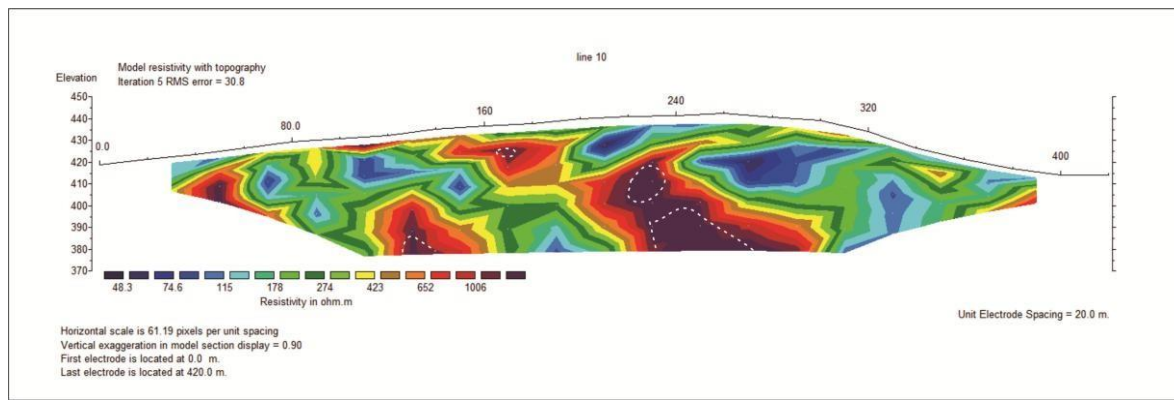


**Figure 12.** Resistivity model on line 10

In **Figure 13**, a 3D interpretation of Andesite rocks (purple) can be shown. The results of this interpretation are based on a combination of 10 line. The trend or direction of the distribution of Andesite rocks is most likely due to a basin that runs along the southeast - northwest. So, it can be assumed that the lava or liquid magma that comes out of volcanic results, moves along the basin, which then forms Andesite rocks. This basin is then covered by weathering of rocks above it and forming sedimentary rocks for a long time.

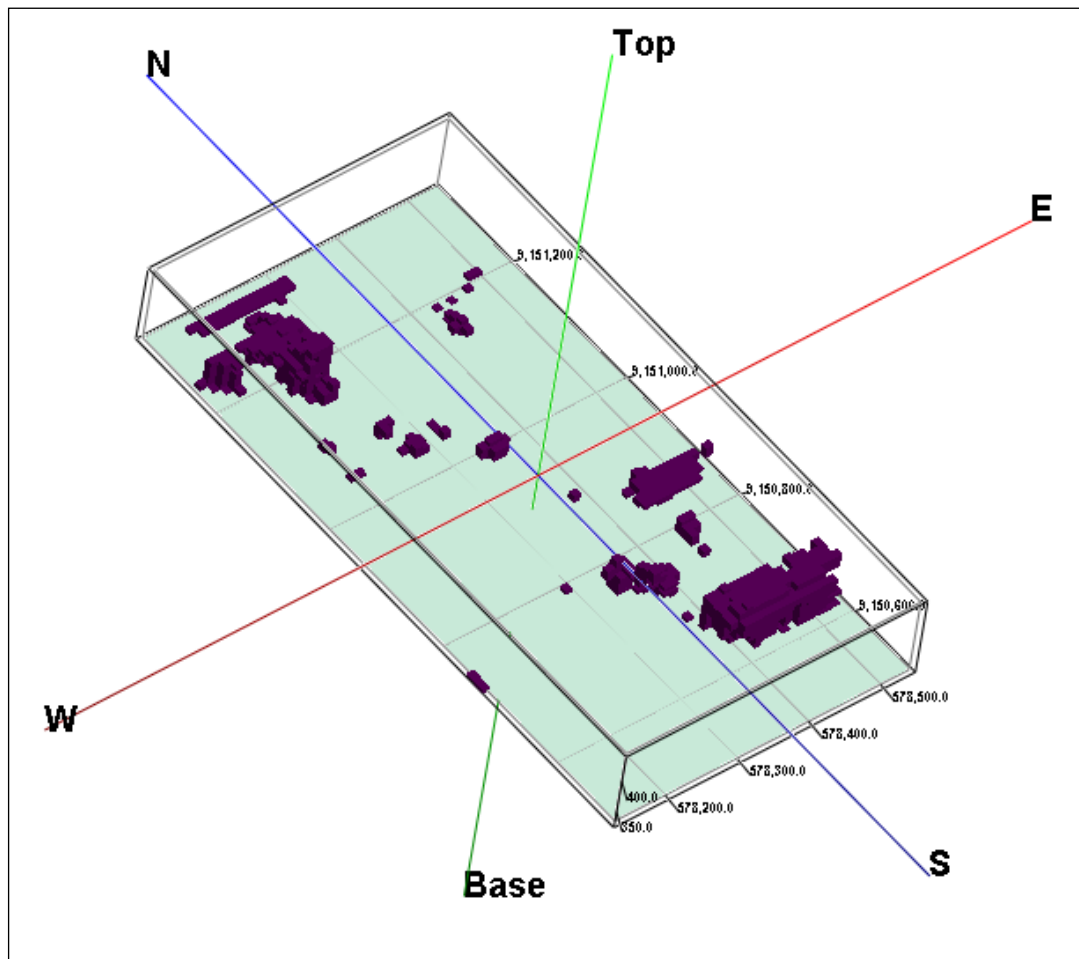


**Figure 13.** 3D Andesite Resistivity Model

**Figure 14** is a combination of measurement paths with 3D interpretation results. In this result, we can predict continuity based on direction and also depth from Andesite rocks or Breccia rocks. The results of this continuity prediction can later be used to estimate the shape of the geoelectric path, if needed in estimating the presence of Andesite and Breccia rocks in other regions.

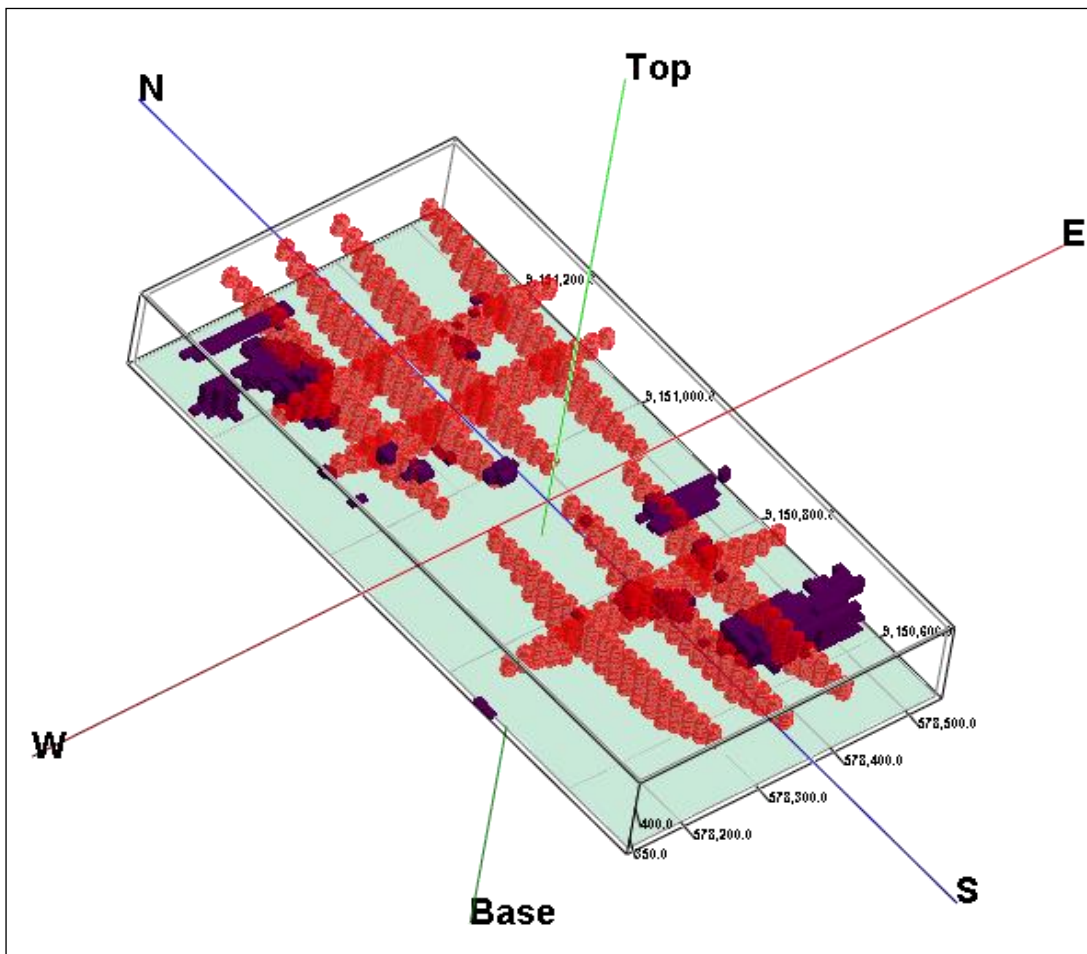


**Figure 14.** 3D model of Andesite resistivity with a red dot is data position

## CONCLUSION

Based on the results of processing and discussion in this study, it can be concluded that the distribution of andesite resistivity values ( $> 1000 \Omega\text{m}$ ) through the cross section of the 3D resistivity model tends to form a trend and extend to the southeast-northwest direction with a depth of about 10-15 meters, and Breccia ( $600-900 \Omega\text{m}$ ) tends to form trends and widen the measuring trajectory. On the other hand, the distribution of andesite rocks and breccia is likely to occur due to the shape of the basin in the trend (southeast-northwest) so that when the eruption occurs, the magma or lava that flows follows the direction of the basin. In addition, the effectiveness of providing information and education to the surrounding community is very good. Because the surrounding community can find out where andesite rocks and breccia widen. So, in this study, the geoelectric application is very helpful for the community in understanding that electricity is not only used for electronic devices but also can be used as a detector for the presence of hybridized rock.

## ACKNOWLEDGMENT

The author would like to thank the relevant parties who have provided support for this research.

## CONFLICTS OF INTEREST

The authors declare no conflict of interest concerning the publication of this article. The authors also confirm that the data and the article are free of plagiarism.

## REFERENCES

Adejumo, R. O., Adagunodo, T. A., Bility, H., Lukman, A. F., & Isibor, P. O. (2018). Physicochemical constituents of groundwater and its quality in crystalline bedrock, Nigeria. *International Journal of Civil Engineering and Technology*, 9(8), 887–903.

Alonso-Pandavenes, O., Torrijo, F. J., Garzón-Roca, J., & Gracia, A. (2023). Early Investigation of a Landslide Sliding Surface by HVSR and VES Geophysical Techniques Combined, a Case Study in Guarumales (Ecuador). *Applied Sciences (Switzerland)*, 13(2). <https://doi.org/10.3390/app13021023>

Anthony, T. B. (2017). Hydrogeochemistry of groundwater within the lateritic profiles over migmatite and pegmatised schist of Ibadan, Nigeria. *Journal of Geology and Mining Research*, 9(4), 28–42. <https://doi.org/10.5897/jgmr2016.0261>

Bronto, S., Asmoro, P., Hartono, G., & Sulistiyyono, S. (2012). Evolution of Rajabasa Volcano in Kalianda Area and Its Vicinity, South Lampung Regency. *Indonesian Journal on Geoscience*, 7(1), 11–25. <https://doi.org/10.17014/ijog.v7i1.132>

Chambers, J., Holmes, J., Whiteley, J., Boyd, J., Meldrum, P., Wilkinson, P., Kuras, O., Swift, R., Harrison, H., Glendinning, S., Stirling, R., Huntley, D., Slater, N., & Donohue, S. (2022). Long-term geoelectrical monitoring of landslides in natural and engineered slopes. *Leading Edge*, 41(11), 768–767. <https://doi.org/10.1190/tle41110768.1>

Chen, X., Zheng, Y., Gao, S., Wu, S., Jiang, X., Jiang, J., Cai, P., & Lin, C. (2020). Ages and petrogenesis of the late Triassic andesitic rocks at the Luerma porphyry Cu deposit, western Gangdese, and implications for regional metallogeny. *Gondwana Research*, 85, 103–123. <https://doi.org/10.1016/j.gr.2020.04.006>

Czinder, B., & Török, Á. (2021). Strength and abrasive properties of andesite: relationships between strength parameters measured on cylindrical test specimens and micro-Deval values—a tool for durability assessment. *Bulletin of Engineering Geology and the Environment*, 80(12), 8871–8889. <https://doi.org/10.1007/s10064-020-01983-9>

Gan, F., Han, K., Lan, F., Chen, Y., & Zhang, W. (2017). Multi-geophysical approaches to detect karst channels underground — A case study in Mengzi of Yunnan Province, China. *Journal of Applied Geophysics*, 136, 91–98. <https://doi.org/10.1016/j.jappgeo.2016.10.036>

Hartmann, L. A., Hoerlle, G., & Renner, L. C. (2024). Extensive two-tier structure and breccia stockwork formation by hydrothermal processes in the first Paraná lava flow covering the Botucatu paleoerg-turned-Guarani Paleoquifer. *Journal of South American Earth Sciences*, 133(May 2023). <https://doi.org/10.1016/j.jsames.2023.104734>

Ibrahim, E., Gultaf, H., Saputra, H., Agustina, L. K., Rahmanda, V., Suhendi, C., Sudibyo, M. R. P., & Rizki, R. (2019). Preliminary Result: Identification of Landslides Using Electrical Resistivity Tomography Case Study Mt. Betung. *Journal of Science and Application Technology*, 2(1), 107–110. <https://doi.org/10.35472/281455>

Khalil, M. A., & Santos, F. M. (2011). Comparative study between filtering and inversion of vlf-em profile data. *Arabian Journal of Geosciences*, 4(1–2), 309–317. <https://doi.org/10.1007/s12517-010-0168-4>

Listyani, R. A. T.-, Prabowo, I. A., & De Jesus, A. A. (2023). Aquifer Potential Analysis Based On Hydrostratigraphy and Geological Lineament In Kokap Region, Kulon Progo, Yogyakarta, Indonesia. *International Journal of Hydrological and Environmental for Sustainability*, 2(2), 50–64. <https://doi.org/10.58524/ijhes.v2i2.197>

Meju, M. A., & Le, L. (2002). Geoelectromagneticexploration For Natural Resources:Models, Case Studies and Challenges. *Surveys in Geophysics*, 23, 133–205.

Mibei, G. (2014). *Presented at Short Course IX on Exploration for Geothermal Resources, INTRODUCTION TO TYPES AND CLASSIFICATION OF ROCKS*. 1–12.

Muthamilselvan, A., Rajasekaran, N., & Suresh, R. (2019). Mapping of hard rock aquifer system and artificial recharge zonation through remote sensing and GIS approach in parts of Perambalur District of Tamil Nadu, India. *Journal of Groundwater Science and Engineering*, 7(3), 264–281. <https://doi.org/10.19637/j.cnki.2305-7068.2019.03.007>

Nugraha, A. S., Darsono, D., & Legowo, B. (2019). Identification of the distribution of andesite rocks in Kalirejo Village, Kokap District, Kulon Progo Regency, Special Region of Yogyakarta based on geoelectrical tomography data. *Journal of Physics: Conference Series*, 1153(1). <https://doi.org/10.1088/1742-6596/1153/1/012019>

Nurwidjanto, M. I., & Yuliyanto, G. (2022). *Application of the HVSR Microtremor Method for Groundwater Aquifer Identification: Case study in Pencitrejo, Terong Village, Dlingo, Bantul, Yogyakarta, Indonesia*. 8(6), 20–23.

Oskooi, B., & Abedi, M. (2015). Magnetic and electromagnetic data interpretation for delineating geological contacts in the Tomelilla area, Sweden. *Arabian Journal of Geosciences*, 8(6), 3971–3984. <https://doi.org/10.1007/s12517-014-1501-0>

Playà, E., Rivero, L., & Himi, M. (2010). Electrical resistivity tomography and induced polarization techniques applied to the identification of gypsum rocks †. *Near Surface Geophysics*, 249–257. <https://doi.org/10.3997/1873-0604.2010009>

Saparun, M., Akbar, R., Marbun, M., Dixit, A., & Saxena, A. (2022). Application of Induced Polarization and Resistivity to the Determination of the Location of Minerals in Extrusive Rock Area, Southern Mountains of Java, Indonesia. *International Journal of Hydrological and Environmental for Sustainability*, 1(3), 108–119. <https://doi.org/10.58524/ijhes.v1i3.137>

Schuessler, J. A., Kämpf, H., Koch, U., & Alawi, M. (2016). Earthquake impact on iron isotope signatures recorded in mineral spring water. *Journal of Geophysical Research: Solid Earth*, 121(12), 8548–8568. <https://doi.org/10.1002/2016JB013408>

Sujitapan, C., Kendall, J. M., Chambers, J. E., & Yordkayhun, S. (2024). Landslide assessment through integrated geoelectrical and seismic methods: A case study in Thungsong site, southern Thailand. *Helijon*, 10(2). <https://doi.org/10.1016/j.heliyon.2024.e24660>

Taira, A. (2001). Tectonic evolution of the Japanese island arc system. *Annual Review of Earth and Planetary Sciences*, 29, 109–134. <https://doi.org/10.1146/annurev.earth.29.1.109>

Tang, L., Zhao, Y., Zhang, S. T., Sun, L., Hu, X. K., Sheng, Y. M., & Zeng, T. (2021). Origin and evolution of a porphyry-breccia system: Evidence from zircon U-Pb, molybdenite Re-Os geochronology, in situ sulfur isotope and trace elements of the Qiyugou deposit, China. *Gondwana Research*, 89, 88–104. <https://doi.org/10.1016/j.gr.2020.08.013>

Thoreau, H. D., & Prayer, Y. I. (2000). *Rocks & Minerals* (p. 38).

Triani, Umam, R., & Sismanto. (2021). 3D Modeling of Subsurface Lawanopo Fault in Southeast Sulawesi, Indonesia Using Grablox and its Consequence to Geohazard. *Indonesian Journal of Geography*, 53(1), 67–77. <https://doi.org/10.22146/IJG.50878>

Watlet, A., Van Camp, M., Francis, O., Poulain, A., Rochez, G., Hallet, V., Quinif, Y., & Kaufmann, O. (2020). Gravity Monitoring of Underground Flash Flood Events to Study Their Impact on Groundwater Recharge and the Distribution of Karst Voids. *Water Resources Research*, 56(4), 1–18. <https://doi.org/10.1029/2019WR026673>

Xu, R., & Wang, L. (2021). The horizontal-to-vertical spectral ratio and its applications. *Eurasip Journal on Advances in Signal Processing*, 2021(1). <https://doi.org/10.1186/s13634-021-00765-z>